

A New Multi-Objective Design for Optimal Placement of Gas Turbines considering Black-start Capability Improvement

Mohammad Reza Esmaili¹, Amin Khodabakhshian², Rahmat-allah Hooshmand²

¹ Esfahan Regional Electric Company, Isfahan, Iran

² Department of Electrical Engineering, Faculty of Electrical Engineering, University of Isfahan, Isfahan, Iran

mr.esmaeli@erec.co.ir, aminkh@eng.ui.ac.ir, Hooshmand_r@eng.ui.ac.ir

Abstract:

Installing new energy sources as redundant black-start (BS) units is an efficient way to enhance the speed of power system restoration, especially when there is a high risk that the available power plants considered as BS units fail to operate. In this regard, this paper provides a new optimal design for the placement of the Gas Turbine (GT) as the redundant energy source to improve the power system performance during both restoration and normal conditions. In doing so, there will be contradictory objective functions to be minimized. Therefore, a multi-objective problem (MOP), as a mixed integer linear programming (MILP), is defined. The Pareto optimal solutions of the MOP are obtained by using a new population-based meta-heuristic technique, called Crow Search Algorithm (CSA). Two power systems are used for the validation of the proposed method. The simulation results show that the system can benefit from this method not only to increase the capability of black-start generation, but also to improve the power system performance in normal conditions. During the restoration process, it also provides the optimal start-up sequences of non-black-start (NBS) units with the optimal transmission paths.

Keywords: Power System Restoration, Black-start Units, Crow Search Algorithm, Multi-objective Design, Pareto Optimal Set.

1. Introduction

The modern power systems are being controlled in a high level of reliability and security. However, different unpredicted events may occur and, in turn, cause to have a wide area of cascading failures and then a blackout for the entire system [1-2]. This can impose huge economic losses and negative social impacts. Therefore, the quick restoration of a power system after a blackout is one of the most important concerns for power system dispatchers, operators and planners [3].

The process of power system restoration includes three stages: preparation, transmission paths reconfiguration and load restoration [4]. In the preparation stage, the black-start units are commissioned, and then transmission paths are connected to crank non-black-start units (NBSU) in order to be started up [5]. The objective of this stage is mainly to maximize the generation capability. In this regard, many

researchers have formulated this objective as an optimization problem [3-6]. In [3] and [5] authors propose an algorithm that formulates generator start-up sequence as a MILP problem. In [3] the firefly algorithm (FA) is used to search the final optimal sequence of NBSUs, transmission paths and load pick up sequence by the aid of renewable energy sources (RES) already installed in power system. In [5] an optimal generator start-up strategy is addressed to find a sequence of starting time for all NBSUs and also to update the generation capability during system restoration. In [6], an initial restoration sequence of generators is obtained by using a mixed integer linear problem (MILP) method. Then, the final restoration sequence is manually acquired by using this initial guess after many trials. A decision making support system is addressed in [7-8] to search the optimal black-start strategy by using a concept of the vague-valued fuzzy measure. In [9] a steady state model is developed to optimize the total generator power output through searching the optimal start-up sequence of NBSUs by using the shortest path decision. In [10], the optimal start-up sequences of generators are designed by applying an algorithm based on Dijkstra method for finding the shortest path during power system

¹ Submission date: 15, 05, 2018

Acceptance date: 17, 11, 2018

Corresponding author: Amin Khodabakhshian,
Department of electrical engineering, Faculty of
electrical engineering, University of Isfahan – Iran
Copyright©2019, University of Isfahan

restoration. In [11], the optimal network reconfiguration was designed into two separately steps. In the first step, the optimal sequence design of generating units was done to maximize the restored generation capability, and in the second step, the optimal transmission path is obtained to crank the generating units. In [12] a combined design of the generating start-up sequence and the transmission path search is presented as an optimization problem and solved by using firefly algorithm.

In all researches published so far, to the best of our knowledge, the selection of black-start unit (BSU) as a starting point of restoration process has been based on the existed units within the power system without performing any design procedure to locate these units. In this regard, although the hydro and Gas Turbine (GT) power plants that are generally considered as the BSUs, due to the high speed of commissioning, it will be possible that these plants do not have enough capabilities to crank NBS units [13]. Some of the hydro power plants are not available because of the insufficient flow of the water or the low level of the stored water behind the dam [14]. Moreover, when the already-installed gas turbine power plants continuously work in the system, there is a high risk that after blackout, the technical problem in fuel system causes to trip the unit or it may not permit to start the unit for restoration preparation [15]. Furthermore, in both gas turbine and hydro power plants, the failure of control systems may stop the process of starting BSU [15-16]. Therefore, considering redundant BSUs is necessary to crank and to increase the speed of restoration [17-19].

There are many situations during the normal condition of a power system that the system should be able to respond to the sudden load demands very quickly. In these cases the new installed GTs that can be started very fast could be one of the best options to help the system increase the generations in the shortest possible time [20-21]. Therefore, it will be more economical to place these units in the locations where the minimum power losses are achieved. They must also justify another important constraint which is the voltage violation during the normal condition. Therefore, the problem of the optimal placement of GTs, as the good candidates for redundant BSUs, will be solved by increasing the capability of black-start generation and also improving the power system performance in normal conditions. In doing so, a multi-objective function is used to obtain the best locations of GTs, the optimal transmission path and the optimal generators start-up

sequences by considering the black-start capability criterion.

There are several techniques for finding the optimal transmission path in a power system including expert system [22], artificial neural networks [23], power transfer distribution factor (PTDF)-based approach [24], linear programming-based approach [25], heuristic approaches [26] and Dijkstra algorithm [27]. Among all these techniques, Dijkstra algorithm has a simpler structure and, therefore, the computational complexity of any proposed design is decreased by using this algorithm [28]. Also, the CPU time of running the proposed optimization model during the optimization process is decreased.

The multi-objective function consists of minimizing the Unavailable Energy Capability (UEC) of the system during the restoration process and also minimizing the voltage deviations of buses and active power losses in transmission system during normal condition to achieve the best Pareto optimal set. Then, a new population-based meta-heuristic technique, called crow search algorithm (CSA) based on fuzzy decision making approach is used to obtain the Pareto optimal solutions. The idea of using CSA is initiated from one of the real and intelligent behavior of storing, hiding and retrieving process of crow's food by themselves [29]. The high level of efficiency, accuracy and robustness to search the Pareto optimal solution and the finding capability of the proposed algorithm make it be a desirable approach for optimizing the MOP addressed in this paper. The main contributions of this paper are as follows:

- Optimal placement of the Gas Turbine (GT) as the redundant energy source to improve the black-start capability,
- Considering all objective functions related to the both restoration and normal conditions simultaneously, and
- Presenting a multi-objective crow search algorithm (MOCSA) for searching the optimal decision variables.

The 39-bus New England power system and a 32-bus power system are employed as two test systems. The simulation results show that not only the proposed method is capable of finding the best locations of the redundant GTs, but also it finds the optimal start-up sequences of NBS units with the optimal transmission paths in order to speed up the restoration process. It also improves the performance of the power system in normal conditions.

The rest of the paper is organized as follows: Section 2 describes the problem formulation. In

Sections 3 and 4, the solution approach (MOCSA) is given to solve the proposed multi-objective problem. Simulation results are given in Section 5 and finally, Section 6 concludes the paper.

2. Problem Formulation

The formulation of the multi-objective model for searching the location of a GT including three objective functions and their constraints is given in this section.

2.1. Objective Functions

The employed objective functions for the proposed multi-objective model are explained in this subsection.

2.1.1. Unavailable Energy Capability Objective Function

The first objective function is used to minimize the total generation capacity (MWh) which is not available after blackout [3] and is given by the following equation [3]:

$$\left\{ \begin{array}{l} \min f_1(x) = \sum_{j=1}^M (P_{j \max} - P_{j \text{start}}) * t_{j \text{start}} \\ \text{St} : \\ T_{j \min} \leq t_{j \text{start}} \leq T_{j \max} \\ t_{j \text{path-opt}} \leq t_{j \text{start}} \\ P_{\text{igen-opt}}(t) \geq P_{j \text{start}}(t), j = 1, 2, \dots, M \end{array} \right. \quad (1)$$

The optimal start-up sequence of NBS units and the optimal locations of GTs are obtained by the optimization of the first objective function. The optimal transmission paths are also determined when the objective function f_1 is calculated. This will be described in the next subsection.

2.1.1.1. Optimal Path Search Algorithm

A minimum spanning tree method is used here to find the shortest paths between two nodes in network and can be shown as a graph [30]. This algorithm, which is an iterative process, has been introduced by W. Dijkstra [30]. A simple example of this algorithm is shown in Fig. 1. In this figure, a shortest path is found between node A (source node) and node E (destination node). The start point of this algorithm is shown by coloured node A (step 1). In the first iteration, the algorithm searches the adjacent node from the source node, which must be the nearest node to the source node (step 2). In the second iteration, the algorithm searches the second nearest node from the source node (step 3). This node must be the nearest node from the first node which was the closest to the

source node. This procedure iteratively continues so that the minimum spanning tree for the source node is found (step 4). This tree gives an optimal path which includes all nodes.

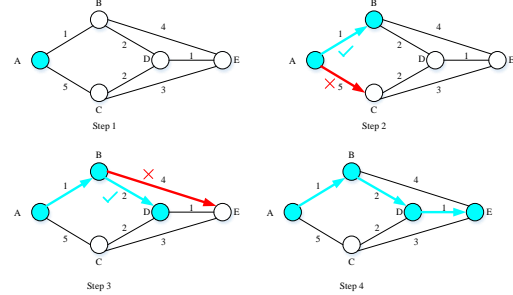


Fig (1): Dijkstra algorithm [30]

2.1.2. Minimization of Active Power Loss

Minimizing the active power loss is formulated as follows [31]:

$$\left\{ \begin{array}{l} \min f_2(x) = \sum_{i=1}^n P_{g_i} - \sum_{j=1}^k P_{l_j} \\ \text{St} : \\ P_{g_i \min} \leq P_{g_i} \leq P_{g_i \max}, i = 1, 2, \dots, n \\ P_{l_j \min} \leq P_{l_j} \leq P_{l_j \max}, j = 1, 2, \dots, k \\ P_{g_i} - P_{l_i} - V_i \sum_{j \in NB_i} V_j (G_{ij} \cos \delta_{ij} + B_{ij} \sin \delta_{ij}) = 0 \\ Q_{g_i} - Q_{l_i} - V_i \sum_{j \in NB_i} V_j (G_{ij} \sin \delta_{ij} + B_{ij} \cos \delta_{ij}) = 0 \end{array} \right. \quad (2)$$

2.1.3. Voltage Violation

The following objective function is given to reduce the voltage violation in all PQ buses [31]:

$$\left\{ \begin{array}{l} \min f_3(x) = \sum_{i=1}^k |V_{ref} - V_i| \\ \text{St} : \\ V_{i \min} \leq V_i \leq V_{i \max}, i = 1, 2, \dots, k \end{array} \right. \quad (3)$$

2.2. Decision Variables

The decision variables are optimally obtained after completing the optimization process in order to achieve the best optimal solution. In the proposed design method, a constrained optimization problem will be described as a multi-objective function and minimized subject to $t_{j \text{start}}^{\min} \leq t_{j \text{start}} \leq t_{j \text{start}}^{\max}$ and $L_{i \min} \leq L_i \leq L_{i \max}$.

The $t_{j \text{start}}$ and L_i are defined as the decision variables and imply all start-up times of NBS units and the location of a GT (redundant BSU) respectively.

2.3. Multi-objective Design

In multi-objective design it is impossible to obtain an optimal solution when all objective functions are simultaneously being optimized, because the objective functions are different and each function is not compromised with other functions. In this condition, a decision maker chooses a “most effective” answer as an optimal solution [32]. Generally, the equation of a MOP can be formulated as follows;

Optimize

$$\mathbf{F}(\mathbf{X}) = [f_1(\mathbf{X}), f_2(\mathbf{X}), \dots, f_K(\mathbf{X})]_{(1 \times K)}^T \quad (4)$$

The vector $\mathbf{X} = [x_1, x_2, \dots, x_n]$ is defined as decision variables and obtained by solving Eqn. (4). Also, this MOP is executed subject to regard the total number of all constraints. These constraints consist of inequality (N_{ieq}) and equality (N_{eq}) constraints as given in Eqns. (5) and (6), respectively.

$$g_i(\mathbf{X}) \leq 0, \quad i = 1, 2, \dots, N_{ieq} \quad (5)$$

$$h_j(\mathbf{X}) = 0, \quad j = 1, 2, \dots, N_{eq} \quad (6)$$

In this study, Eqns. (5) and (6) include all equality and inequality constraints given in Eqns. (1), (2) and (3) which are the starting times of NBSUs and the generation capability of BSUs, active and reactive power balance and also the voltages of buses.

Generally, the proposed MOP is optimized by storing a group of most desirable answers in a repository and renewing the group at any iteration [33]. In this technique, the best acquired answers are defined as non-dominated answers or Pareto optimal set. An answer can be determined as a Pareto optimal set if and only if Eqn. (7) is satisfied.

$$\begin{aligned} & \forall k \in \{1, 2, 3, \dots, K\}: \forall \mathbf{X} \in \mathcal{X} - \{\mathbf{X}^*\}, f_k(\mathbf{X}^*) \leq f_k(\mathbf{X}) \\ & \& \\ & \exists m \in \{1, 2, 3, \dots, K\}: f_m(\mathbf{X}^*) < f_m(\mathbf{X}) \end{aligned} \quad (7)$$

In Eqn. (7) \mathbf{X}^* is defined as the Pareto optimal set of the possible search space of \mathcal{X} . It also implies that enhancing one objective function by an allowable answer will be gained by degrading the optimal solution of at least one of the other objective functions.

2.4. Best Acceptable Solution

In the optimization process, it is required that a solution be considered between all non-dominated answers of the Pareto optimal set as the best allowable answer [33]. In this paper, a fuzzy mechanism is used for three objective

functions (f_1, f_2, f_3) because their values are not precise. In this regard, a fuzzy membership function is defined for achieving the most desirable answer. For all individual recorded in repository, the following equation is formulated [33]:

$$\mu_{f_i}(x) = \begin{cases} 0 & f_i(X) \geq f_i^{\max} \\ \frac{f_i^{\max} - f_i(X)}{f_i^{\max} - f_i^{\min}} & f_i^{\min} \leq f_i(X) \leq f_i^{\max} \\ 1 & f_i(X) \leq f_i^{\min} \end{cases} \quad (8)$$

where f_i^{\max} and f_i^{\min} are described as the maximum and minimum limits of each objective function respectively. These amounts are calculated by comparing with the values acquired by the single optimization of each objective function.

The normalization of the membership of the recorded individuals could be done according to the following equation [34]:

$$N_\mu(X_i) = \frac{\sum_{k=1}^h w_k \times \mu_{f_k}(X_i)}{\sum_i^d \sum_k^h w_k \times \mu_{f_k}(X_i)} \quad (9)$$

where h, d, w_k are the total number of objective functions, the number of Pareto optimal answers in repository and the weight of K_{th} objective function respectively. Finally, the best compromise solution is considered as the solution which has the maximum N_μ .

2.5. Repository Size Control

One of the main factors in the design of any evolutionary optimization approach is to control its repository's size [35-36]. In this paper, a fuzzy clustering technique is used to control the size of the repository without changing its characteristics [35]. In doing so, each solution of the repository is defined as a cluster with definite radius. Neighbor clusters are combined until the proper repository size is achieved. In the combining stage, the member with the higher membership value of combined clusters is chosen to be recorded in the repository. The flowchart of the whole mechanism using fuzzy based clustering is given in Appendix.

3. Crow Search Algorithm

The idea of crow search algorithm (CSA) was firstly created from one of the real and intelligent behavior of crows by A. Askarzadeh in 2016 [29]. This algorithm formulates the storing, hiding and retrieving process of crow's food by themselves. The full details of CSA are given in [29].

One of the most important specifications of meta-heuristic algorithms is satisfying a good balance between diversification and intensification [37]. In CSA, intensification and diversification are principally balanced by the parameter of awareness probability (AP). By decreasing the value of AP, the searching process will go into a local area in CSA where a current good solution is obtained in this area. On the other hand, increasing the value of AP conducts searching process in CSA into the global area (randomization). Therefore, diversification is increased by applying the large values of AP.

4. Implementation of CSA in Multi-objective Design for Optimal Placement of GTs

Now, the design procedure for implementation of CSA in multi-objective design is described as follows:

Step 1: Determine the required data which are flock size of crows (N), flight length (fl), awareness probability (AP), maximum iteration, and Pareto archive dimension.

Step 2: Generate the initial random population of crow's position and their memories.

Step 3: Compute the value of objective functions for each crow by solving Equation 4.

Step 4: Investigate the constraints of the problem by using Eqns. (1), (2) and (3). If the constraints are not satisfied, consider a high value of penalty for objective functions related to the current crow, otherwise, ignore it.

Step 5: Search the non-dominated solutions among the possible solutions and record them in the Pareto repository according to Eqns. (8) and (9).

Step 6: Check the repository size. If the size of repository is more than the maximum predefined size, remove the extra member with fuzzy based clustering mechanism.

Step 7: Generate the new population of crow's position by using Eqns. (10) and (11).

Step 8: Check the feasibility of the new population of crow's position. If the new position is possible, go to step 9. Otherwise, go to step 7.

Step 9: Compute the value of objective functions for each crow by solving Equation 4.

Step 10: Investigate the constraints of the problem by using Eqns. (1), (2) and (3). If the constraints are not satisfied, consider a high value of penalty for objective functions related to the current crow, otherwise, ignore it.

Step 11: Update the repository by replacing the new non-dominated solutions according to Eqns. (8) and (9).

Step 12: Check the repository size. If the size of repository is more than maximum predefined size, remove the extra member with fuzzy based clustering mechanism.

Step 13: Check the convergence criterion. If the maximum iteration number is reached, stop the execution of the algorithm. Otherwise go back to step 7.

The flowchart of the above-mentioned steps is given in Fig. 2.

5. Simulation Results

In this section, the proposed method is performed on two different power systems to show its efficient performance during restoration and normal conditions.

5.1. The 39-bus New England Power System

The single line diagram of the 39-bus New England power system is depicted in Fig. 3 and its information can be found in [38]. This system is segmented into two subsystems only at restoration condition according to [3], and each subsystem must have at least one black-start unit [39]. Therefore, the number of already installed BSUs is assumed to be 2, which are G6 and G10 [3, 5]. As mentioned in section 1, it is essential that the redundant BSUs (GTs) be considered for each power system, and their optimal locations are obtained.

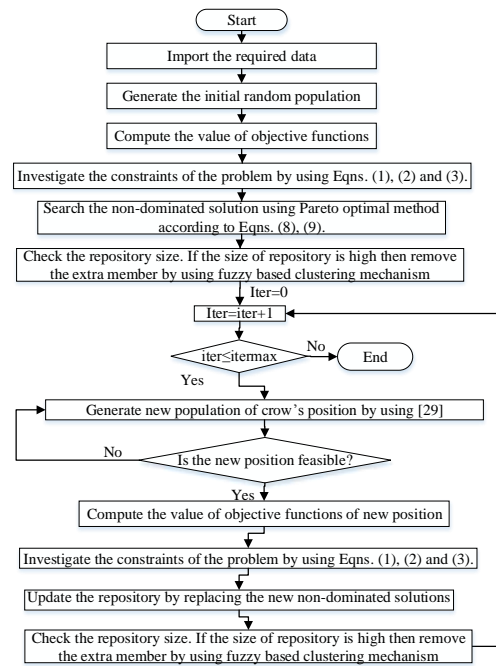
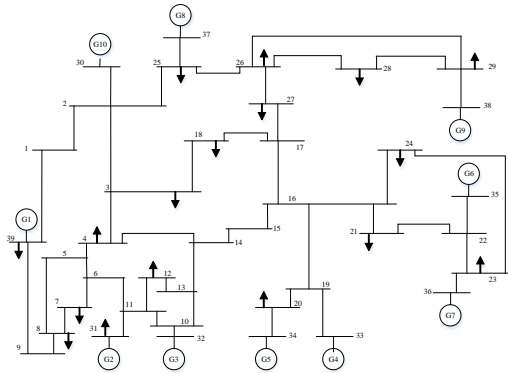


Fig (2): Flowchart of application of CSA on multi-objective design


Fig (3): IEEE 39-bus power system [37]

Now, the proposed design procedure is performed in two stages. First, the single objective design is done to specify and to use the limit values of three objective functions f_1 , f_2 and f_3 (Eqns. (1), (2) and (3)) for the second stage (multi-objective design). Then, the multi-objective design is carried out to determine the optimal solution (or optimal decision variables), which are the start-up times of NBS units and the locations of GTs. The required data of generators for black-start process are given in Table 1 according to [5]. In this table, T_{cp} refers to the cranking time for generator to start to ramp up for connecting with system, and R_r is the rate of generator ramping.

Table (1): Characteristics of generating units in 39-bus system [4]

unit	Type	P_{max} (MW)	P_{start} (MW)	R_r (MW/hr)	T_{max} (min)	T_{min} (min)
G1	Coal	572.9	5.5	215	N/A	40.
G2	Nuc.	650	8	246	N/A	N/A
G3	Nuc.	632	7	236	120	N/A
G4	Coal	508	5	198	N/A	70
G5	Coal	650	8	244	60	N/A
G6	Nuc.	560	0	214	N/A	N/A
G7	Coal	540	6	210	N/A	N/A
G8	Nuc.	830	13.2	346	N/A	N/A
G9	Nuc	1000	15	384	N/A	N/A
G10	Hyd.	250	0	162	N/A	N/A

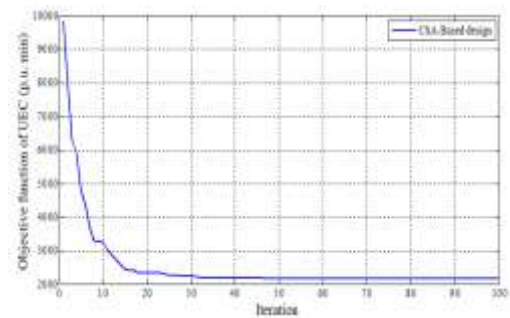
5.1.1. Single Objective Design

In this part, single objective design is performed by using CSA algorithm. The extracted data of this part are used as the limits for the multi-objective approach.

5.1.1.1. Restoration Condition

In this subsection, the objective function f_1 (Eqn. (1)) is minimized by using CSA so that all optimal start-up times of NBS units and the best

locations of GTs (redundant BSUs) are obtained and the results are given in Table 2. The convergence curve of f_1 is also shown in Fig. 4. The last row of Table 2 shows the best value of the objective function f_1 used for the limits considered in multi-objective method. By using the optimal search path algorithm explained in section 2.1.1.1, the optimal start-up sequences of NBSU units are obtained and given in Table 2. In this regard, each subsystem includes one redundant BSU and four NBSUs. . It should be mentioned that the capacity of each gas turbine is selected to be 50 MW because the total amount of power needed for starting all NBS units (P_{start}) in each subsystem is 50 MW.


Fig (4): CSA-based convergence curve of UEC
Table (2): Optimal design of generators start-up process using CSA-based design considering redundant BSU

Subsystem 1	Gen	G10	G1	G2	G8	G9	BSU
	BSU	-	-	-	-	-	-
NBSU	√	√	√	√	√	√	-
t_{start} (min)	25	40	40	30	40	40	15
Location of BSU	-	-	-	-	-	-	Bus 3
Subsystem 2	Gen	G4	G3	G5	G6	G7	BSU
	BSU	-	-	-	-	-	-
NBSU	√	√	√	√	√	√	-
t_{start} (min)	70	40	30	30	35	35	15
Location of BSU	-	-	-	-	-	-	Bus 16
Value of UEC	2334.9						

The colored optimal path of cranking power for all NBSUs is depicted in Fig. 5. In this figure, the sequence of start-up for all NBSUs is determined by a specific color. For more clarification, the details of these paths are given in Table 3.

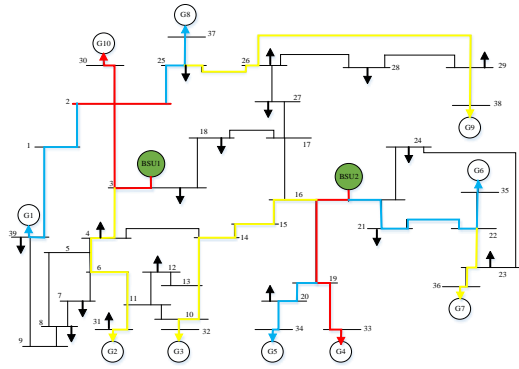


Fig (5): Optimal generator start-up of IEEE 39 bus power system using redundant BSU

As mentioned before, G6 and G10 have been considered as main BSUs. A comparison is performed between two different cases where the system is equipped with new GTs as redundant BSUs and the case where new GTs are not installed. The results are presented in Table 4. The results given in this table show that the value of UEC for all cases is desirably decreased when new GTs are used when either G6 or G10 fails to operate. For example, in case 1 when G6 fails to operate, the value of UEC by

using new GTs (2309.9 min. p.u.) is lower than the ones without new GTs (2870.60 min. p.u.). For the worst situation (case 3) when both G6 and G10 fail to operate, by using new GTs as redundant BSU units, the value of UEC is 2334.90 min. p.u., which means that the black-start process is successfully performed.

Table (3): The optimal cranking power paths of NBSUs in New England power system

Location of redundant BSU	NBS unit	optimal cranking power paths
Bus 3	G1	Bus: 3→2→1→39
Bus 3	G2	Bus: 3→4→6→31
Bus 3	G8	Bus: 3→2→25→37
Bus 3	G9	Bus: 3→2→25→26→29→38
Bus 3	G10	Bus: 3→2→30
Bus 16	G3	Bus: 16→15→14→13→10→32
Bus 16	G4	Bus: 16→19→33
Bus 16	G5	Bus: 16→19→20→34
Bus 16	G6	Bus: 16→21→22→35
Bus 16	G7	Bus: 16→21→22→23→36

Table (4): Effect of GTs as the redundant BSUs in black-start process during different cases

Gen. unit		1	2	3	4	5	6	7	8	9	10
With GTs	t_{start}	40	40	40	70	30	30	35	30	40	15
	value of UEC	2309.90									
Without GTs	t_{start}	40	50	50	70	55	55	60	30	40	15
	value of UEC	2870.60									
With GTs	t_{start}	40	40	40	70	45	15	30	30	40	25
	value of UEC	2320.5									
Without GTs	t_{start}	65	60	55	70	45	15	30	55	55	55
	value of UEC	3948.7									
With GTs	t_{start}	40	40	40	70	30	30	35	30	40	25
	value of UEC	2334.90									
Without GTs	t_{start}	∞	∞	∞	∞	∞	∞	∞	∞	∞	∞
	value of UEC	∞									

5.1.1.2. Normal Condition

In this subsection, the values of objective functions f_2 and f_3 (Eqns. (2) and (3)) are separately minimized by executing the CSA based power flow analysis. Optimizing f_2 and f_3 gives the locations of GTs during the steady state condition. Figures 6 and 7 show the convergence curves of f_2 and f_3 respectively. The optimal values of these curves are shown in Table 5. The best locations of GTs and the minimum value of the related objective function

are presented in this table. The third column of Table 5 gives different locations for GTs (bus 8 for f_2 and bus 21 for f_3) because of having the conflict between the single objective functions during the optimization process. Also, the extracted data of active power loss (0.4164 p.u.) and voltage violation (2.2513 p.u.) given in this table are chosen as the limits for the multi-objective approach. As expected and given in Tables 2 and 5, the location of GTs are different

because different objective functions have been used in different conditions.

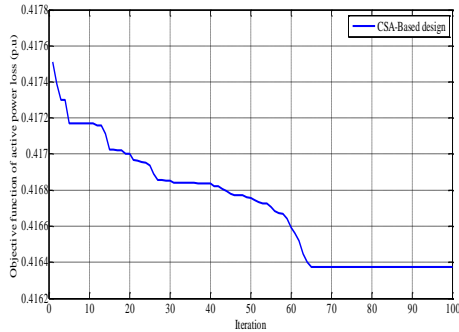


Fig (6): CSA-based convergence curve of active power loss in steady state condition

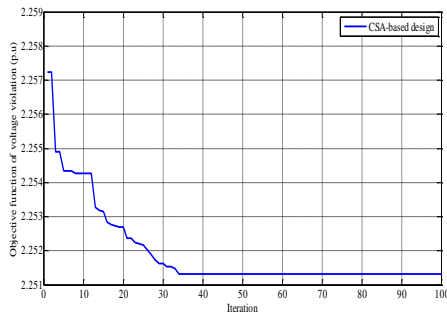


Fig (7): CSA-based convergence curve of voltage violation in steady state condition

Table (5): Optimal design of objective function during CSA-based power flow analysis

Objective function	Value of objective function	Locations of New GTs
Active power loss (p.u)	0.4164	Bus 8
Voltage violation (p.u)	2.2513	Bus 21

To show the efficiency of Dijkstra algorithm during searching the optimal cranking paths, a comparative analysis between this algorithm and heuristic algorithms is performed. The results shown in Table 6 imply that the CPU time of Dijkstra algorithm (1105 s) for finding the optimal paths is less than the heuristic algorithms including PSO (1240 s) and CSA (1235 s). Also, executing the program in 100 times, Dijkstra algorithm gives the best cranking paths in 95% of the total trials which is much more than the other algorithms; 87% and 85% for CSA and PSO algorithms respectively.

Table (6): Comparison of the results for different algorithms to obtain optimal path

Criteria	Algorithm		
	Dijkstra-based	CSA-based	PSO-based
CPU time (s)	1105	1235	1240
Number of iteration	32	43	47
No. global solution	95	87	85

5.1.1.3. Multi-objective Design

In this section, the CSA based multi-objective design is executed to attain the optimal decision variables (all optimal start-up times of NBS units and the best locations of GTs) by the coordinated optimization of three objective function f_1 , f_2 and f_3 ((Eqns. (1) , (2) and (3)), and results are shown in Table 7. The Pareto optimization curve is displayed in Fig. 8 in which the red star is assigned as the best compromise solution. According to Table 7, the optimal values of objective functions are more than the optimal ones obtained in single objective design (see Tables 2 and 5). This is because of the fact that all objective functions are simultaneously minimized in the multi-objective design. Table 6 also shows that the value of UEC (2522.37 p.u. min) obtained in MOP design is lower than the ones obtained in Table 4 for cases when new GTs are not used. This means that the multi-objective optimization method has a desirable performance in black-start process. Also, the start-up times of G2, G3, G5 and G7 in multi-objective design are less than the cases where new GTs are not used as given in Table 4.

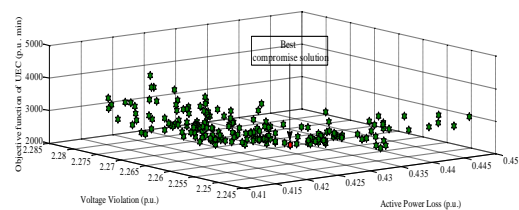


Fig (8): Pareto curve of CSA-based multi-objective method

Table (7): Optimal multi-objective design using CSA-based optimization

Subsystem 1	Gen	G10	G1	G2	G8	G9	redundant BSU
	BSU	-	-	-	-	-	√
	NBSU	√	√	√	√	√	-
	t_{start} (min)	35	40	30	35	55	15
	Location of BSU	-	-	-	-	-	Bus 5

Subsystem 2	Gen	G4	G3	G5	G6	G7	redundant BSU
	BSU	-	-	-	-	-	√
	NBSU	√	√	√	√	√	-
	t_{start} (min)	70	45	35	35	25	15
	Location of BSU	-	-	-	-	-	Bus 24
Value of UEC (p.u . min)		2522.37					
Active power loss (p.u)		0.426					
Voltage violation (p.u)		2.2570					

It should be noted that all objective functions are weighted by the same coefficient ($w_1=w_2=w_3=0.33$). w_1 , w_2 and w_3 show the weights of three objective functions of UEC, active power loss and voltage violation, respectively. In order to show the reason of choosing these weights, two different solutions with different weights are used for IEEE 39-bus power system and the results are shown in Table 8. As can be seen in this table, the value of UEC for solution 2 (2522.3 pu.m) is very close to solution 1 (only 0.8% difference). However, the values of active power loss and voltage violation in solution 2 (0.426 pu and 2.257 pu) have been decreased in comparison with solution 1 by 7% and 1.2 % respectively. This means that considering similar weight coefficients for objective functions in multi-objective design desirably decreases the active power loss and voltage violation in normal operation and also maintains the value of UEC close to solutions 1 and 2.

Table (8): Results of different solution of GT optimal placement for IEEE 39 bus power system

Solution	Value of UEC (pu.min)	Value of voltage violation (pu)	Value of active power loss (pu)
$solution1: \begin{cases} w_1 = 0.7 \\ w_2 = 0.15 \\ w_3 = 0.15 \end{cases}$	2500.5	2.284	0.456
$solution1: \begin{cases} w_1 = 0.33 \\ w_2 = 0.33 \\ w_3 = 0.33 \end{cases}$	2522.3	2.257	0.426

Another analysis is also performed for verifying the normal condition. The active power loss and the voltage violation of the system are computed before and after installation of new GTs. The results are given in Table 9. As can be seen in this table the active

power loss and voltage violation are efficiently declined when new GTs are used. For example, the active power loss after using new GTs decreases about %7.66 for case 3 (max load). Also, the value of voltage violation decreases about %1.47.

To assess the performance of CSA algorithm, a comparison is also done between CSA, particle swarm optimization (PSO) and genetic algorithm (GA) methods for three cases of the best, average and worst solutions. The results of this comparative analysis are presented in Table 10. As shown in this table, the proposed CSA provides more desirable results in comparison with other two algorithms. For example, UEC amount in “best solution” part is 2522.37 for CSA method while this amount is 2528.45 for PSO and 2533.71 for GA. Executing the program in 100 times, CSA achieves to the best solution in 91% of the total trials which is much more than the other algorithms; 85% and 78% for PSO and GA algorithms respectively. This result shows the robustness of the proposed algorithm. Moreover, CPU time of CSA is lower than that of PSO because it is minimized to obtain the optimal solution in less iteration, needs fewer members, and it also avoids from being trapped in the local solution. The amount of the standard deviation is also lower for CSA than the others. As can also be seen in Table 10, the number of global solutions in this algorithm is higher than the others, and its standard deviation of N_{μ} has lower value in comparison with other algorithms.

Table (9): Extracted data during power flow analysis for normal condition

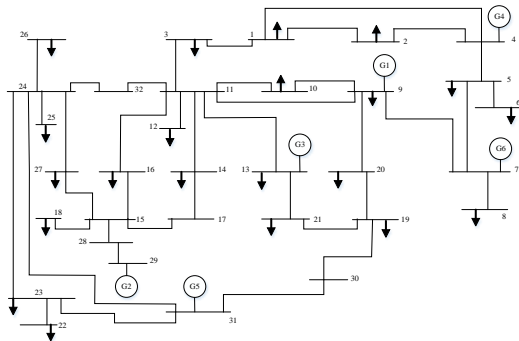
Objective function		Active power loss	Voltage violation
Case 1 (min load)	Without new GTs	0.4214	2.2513
	With new GTs	0.4135	2.2291
Case 2 (mid load)	Without new GTs	0.4294	2.2587
	With new GTs	0.4182	2.2320
Case 3 (max load)	Without new GTs	0.4592	2.2908
	With new GTs	0.4265	2.2570

Table (10): Comparison of the results obtained by different algorithms considering multi-objective problem for 100 trials.

Solution	Criteria	Algorithm		
		CSA	PSO	GA
Best solution	active power loss	0.426	0.429	0.431
	voltage deviation	2.257	2.263	2.264
	UEC	2522.37	2528.45	2533.71
	N_{μ}	0.0343	0.0312	0.0295
Average solution	active power loss	0.4255	0.433	0.43
	voltage deviation	2.375	2.395	2.44
	UEC	2531.41	2536.50	2540.05
	N_{μ}	0.0335	0.0305	0.0287
Worst solution	active power loss	0.431	0.437	0.439
	voltage deviation	2.45	2.48	2.55
	UEC	2533.30	2541.33	2543.65
	N_{μ}	0.0319	0.03	0.028
SD		0.0005100	0.0005500	0.00058
No. global solution		91	85	78
CPU time (s)		720.5	735.2	801.5

5.2. Case2: 32-bus Power System

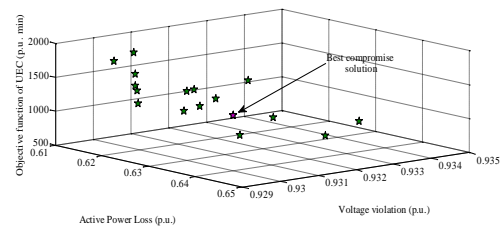
In this subsection, a 32-bus power system is considered to apply the proposed method. The required data and the single line diagram of this power system are given in Table 10 and Fig. 9, respectively. In this network, G4 and G5, which are already installed to supply electrical energy, are also considered as BS units. As reported in [17] there is a high risk that these two units fail during the restoration process. Therefore, the proposed multi-objective design method is applied to this system to find the location of the redundant BSU that should be installed in the system as well as determining the optimal starting times of NBSUs. Like 39-bus power system this power system is also divided into two subsystems as shown in Table 11.


Fig (9): Single line diagram of 32-bus power system
Table (11): Characteristics of generating units in 32-bus power system

Generating unit	G1	G2	G3	G4	G5	G6
Type of unit	steam	steam	steam	Gas	Gas	Gas
P_{\max} (MW)	800	800	830	780	270	420
P_{start} (MW)	12	12	14	8	5	7
R_r (MW/min)	5	5	4	10	10	7
T_{\max} (min)	90	90	120	N/A	N/A	N/A
T_{\min} (min)	30	30	30	N/A	N/A	N/A

The results of this analysis are given in Table 12. The Pareto optimization curve is depicted in Fig. 10. In this figure, the best compromise solution is optimally obtained and shown by the magenta star considering $i = 1, 2, 3$. The value of w_i in Eqn. (9), as mentioned for 39-bus power system, is also considered to be equal ($w_i = 0.33$) for this system.

The optimal cranking power paths of NBSUs are given in Table 13 according to the obtained data of CSA-based multi-objective design. As can be seen in Tables 11 and 12, redundant BSUs (new GTs) are optimally located in buses 14 and 17 in subsystems 1 and 2 respectively. Since it is assumed that the maximum amount of power needed for starting all NBS units (P_{start}) in each subsystem is 50 MW, the capacity of each new GT is selected to be 50 MW.


Fig (10): Pareto curve of CSA-based multi-objective method

A power flow analysis is carried out to display the effective locations of new GTs in satisfying the operating constraints according to the proposed method. In this analysis, three different cases of minimum load, medium load and maximum load are chosen. The active power loss and the voltage violation of the system are calculated before and after installation of new GTs. The results are shown in Table 14. As can be seen in this table the active power loss and voltage violation are efficiently declined when new GTs are used. For example, the active power loss after using

new GTs is 0.6587 (p.u.) for case 3 (max load). If these new GTs are installed in the system, this value will decrease about %2.17. Also, the value of voltage violation decreases about %2.26.

Table (12): Optimal multi-objective design using CSA for 32-bus power system

Subsystem 1	Gen	G1	G3	G4	G6	GT1
	BSU	-	-	-	-	-
NBSU	√	√	√	√	√	-
t_{start} (min)	30	30	20	15	15	
Location of BSU	-	-	-	-	-	Bus 14
Subsystem 2	Gen	G2		G5		GT2
	BSU	-	-	-	-	√
	NBSU	√	√	√	√	-
	t_{start} (min)	30	30	10	10	15
	Location of BSU	-	-	-	-	Bus 27
Value of UEC (p.u. min)		963.30				
Active power loss (p.u)		0.6258				
Voltage violation (p.u)		0.9316				

Table (13): The optimal cranking power paths of NBSUs

Location of BSU	NBS unit	optimal cranking paths
Bus 14	G1	Bus: 14→11→9
Bus 14	G3	Bus: 14→11→13
Bus 14	G4	Bus: 14→11→3→1→4
Bus 14	G6	Bus: 14→11→9→7
Bus 27	G2	Bus: 27→15→28→29
Bus 27	G5	Bus: 27→24→31

Table (14): Obtained data of objective functions during power flow analysis

Objective function		Active power loss	Voltage violation
Case 1 (min load)	Without GTs	0.6298	0.9463
	With new GTs	0.6030	0.9241
Case 2 (mid load)	Without GTs	0.6537	0.9666
	With new GTs	0.6250	0.9365
Case 3 (max load)	Without GTs	0.6733	0.9733
	With new GTs	0.6587	0.9513

6. Conclusions

In this paper, a new multi-objective design was proposed to find the best locations of GTs as the redundant black-start units. During the optimization process, the optimal generators start-up sequences with the optimal transmission paths are also determined. Unavailable energy capability, total active power loss and voltage deviation are considered as the objective functions and are minimized by using the CSA algorithm. The Pareto optimization method was applied to optimize the multi-objective problem and a group of answers, called Pareto optimal solution was obtained. The simulations results showed that active power loss and voltage violation are efficiently declined when new GTs are added to the system. Also, the unavailable energy capability decreased when these GTs were applied as redundant BSUs. It was also found that the CSA given in this paper has a high speed in convergence, especially when compared with other meta-heuristic algorithms.

References

- [1] S.A. Nezam-Sarmadi, S. Nourizadeh, S. Azizi, A. M. Ranjbar, "A power system build-up restoration method based on wide area measurement systems," European Transactions on electrical Power, Vol. 21, pp. 712-720, 2011.
- [2] W. Ye, F. Xinyan, Y. Zheng, "Optimal power grid black-start using fuzzy logic and expert system," European Transactions on electrical Power, Vol. 19, pp. 969-977, 2009.
- [3] A. M. El-Zonkoly, "Renewable energy sources for complete optimal power system black-start restoration," IET Gener Transm Distrib, Vol. 9, No. 6, pp. 531-539, 2015.
- [4] D.H. Kim, Y.T. Yoon, S.S. Lee, S.K. Lee, "Power system restoration plan using the characteristics of scale-free networks," European Transactions on electrical Power, Vol. 18, pp. 809-819, 2008.
- [5] W. Sun, C.C. Liu, L. Zhang, "Optimal Generator Start-Up Strategy for Bulk Power System Restoration," IEEE Trans Power Syst, Vol. 26, pp. 1357-1366, 2011.
- [6] L.H. Fink, K.L. Liou, C.C. Liu, "From generic restoration actions to specific restoration strategies," IEEE Trans Power Syst, Vol. 10, pp. 745-751, 1995.
- [7] S. Zeng, Z. Lin, F. Wen, G. Ledwich, "A new approach for power system black-start decision-making with vague set theory," Int J Electr Power Energy Syst, Vol. 34, pp. 114-120, 2012.
- [8] W.J. Liu, Z. Lin, F. Wen, G. Ledwich,

- “Intuitionistic fuzzy Choquet integral operator-based approach for black-start decision-making,” *IET Gener Transm Distrib*, Vol. 6, No. 5, pp. 378-386, 2012.
- [9] E. Lu, N. Wang, Z. Qin, H. Liu, Y. Hou, “Black-start strategy for power grids including fast cut thermal power units,” *Proc. IEEE Power and Energy Society General Meeting*, pp. 1-5, 2013.
- [10] C. Liu, M. Wu, Y. Deng, “Start-up sequence of generators in power system restoration avoiding the backtracking algorithm,” *Proc. IEEE Power and Energy Society General Meeting*, pp. 1-5, 2013.
- [11] C. Zhang, Z. Lin, F. Wen, G. Ledwich, Y. Xue, “Two-stage power network reconfiguration strategy considering node importance and restored generation capacity,” *IET Gener Transm Distrib*, Vol. 8, pp. 91-103, 2014.
- [12] A. El-Zonkoly, H. Desouki, A. Farghaly, “Firefly based approach for optimal power system black-start restoration,” *Proc. EPE*, pp. 11-16, 2014.
- [13] T. YU, J. Tong, K. W. Chan, “Study on micro-turbine as a back-up power supply for power grid black-start,” *IEEE Power and Energy Society General Meeting*, 2009.
- [14] How hydroelectric energy works. [Online], http://www.ucsusa.org/clean_energy/our-energy_choices/renewable-energy/how-hydroelectric-energy.html
- [15] D. Grace, T. Christiansen, “Risk-based assessment of unplanned outage events and costs for combined-cycle plants,” *Journal of Engineering for gas turbines and power*, Vol. 135, No. 2, pp. 1-7, 2013.
- [16] L. C. Ribeiro, L. Oliveira, E. L. Bonaldi, L. Silva, C. P. Salomon, J. G. Silva, G. L. Torres, “Automatic system for failure detection in hydro-power generators,” *Journal of Power and Energy Engineering*, Vol. 2, pp. 36-46, 2014.
- [17] Black-start service business rules. [Online], http://www.ieso.ca/Documents/consult/se16/se16_DACP-SWG-20060216-pjm-blackstart.pdf
- [18] W. Sun, C. Liu, S. Liu, “Black start capability assessment in power system restoration,” *IEEE Power and Energy Society General Meeting*, pp. 1-7, 2011.
- [19] Y. Chou, C. Liu, Y. Wang, C. Wu, C. Lin, “Development of a Black Start Decision Supporting System for Isolated Power Systems,” *IEEE Trans. Power Syst*, Vol. 28, No. 3, pp. 2202-2210, 2013.
- [20] N. Jenkins, J.B. Ekanayake, G. Strbac, “Distributed generation,” *The Institution of Engineering and Technology*, London, United Kingdom, 2010.
- [21] A. Cano, F. Jurado, “optimal location of biomass-fuelled gas turbines in an electric system,” *IEEE power engineering society meeting*, pp. 1-6, 2006.
- [22] C. C. Liu, S. J. Lee, S. S. Venkata, “An expert system operational aid for restoration and loss reduction of distribution systems,” *IEEE Trans. Power Syst.*, Vol. 3, No. 2, pp. 619-626, 1988.
- [23] A. S. Bretas, A. G. Phadke, “Artificial neural networks in power system restoration,” *IEEE Trans. Power Delivery*, Vol. 18, No. 2, pp. 1181-1186, 2003.
- [24] C. Wang, V. Vittal, S. Kolluri, S. Mandal, “PTDF-based Automatic Restoration Path Selection,” *IEEE Trans. Power Systems*, Vol. 25, No. 3, pp. 1686-1695, 2010.
- [25] W. Sun, C. C. Liu, “Optimal Transmission Path Search in Power System Restoration,” *IREP Symposium-Bulk Power System Dynamics and Control –IX (IREP)*, pp. 1-5, 2013.
- [26] Y. Fukuyama, H. Endo, Y. Nakanishi, “A hybrid system for service restoration using expert system and genetic algorithm,” *Intell. Syst. Appl. Power Syst.*, pp. 394–398, 1996.
- [27] D. Wang, L. Song, Y. Zhang, Z. Lu, H. Li, “The Bi-level programming optimization method of extended black-start schemes considering safety factors during restoration process,” *China International Conference on Electricity Distribution*, pp. 1-5, 2016.
- [28] T. D. Sudhakar, N. S. Vadivoo, S. M. R. Slochanal, S. Ravichandran, “Supply restoration in distribution networks using Dijkstra’s algorithm,” *International Conf. on Power System Technology (POWERCON)*, pp. 640-645, 2004, 640-645.
- [29] R. Askarzadeh, “A novel meta-heuristic method for solving constrained engineering optimization problems: Crow search algorithm,” *Computers and Structures*, Vol. 169, pp. 1-12, 2016.
- [30] E. W. Dijkstra, “A note on two problems in connection with graph,” *Numerische mathematic*, Vol. 1, pp. 269-271, 1959.
- [31] R. H. Liang, J. C. Wang, Y. T. Chen, W. T. Tseng, “An enhanced firefly algorithm to multi-objective optimal active/reactive power dispatch with uncertainties consideration,” *Int J Electr Power Energy Syst*. Vol. 64, pp. 1088-1097, 2014.
- [32] T. Niknam, M. Bornapour, A. Ostadi, A. Gheisari, “Optimal planning of Molten Carbonate Fuel Cell Power Plants at distribution networks considering Combined

Heat, Power and Hydrogen production,” Journal of Power Sources, Vol. 239, pp. 513-526, 2013.

- [33] M. Bornapour, R. Hooshmand, “An efficient scenario-based stochastic programming for optimal planning of combined heat, power, and hydrogen production of molten carbonate fuel cell power plants,” Energy, Vol. 83, pp. 734-748, 2015.
- [34] A. Khodabakhshian, M. R Esmaili, M. Bornapour,” Optimal coordinated design of UPFC and PSS for improving power system performance by using multi-objective water cycle algorithm,” Int J Electr Power Energy Syst, Vol. 83, pp. 124-133, 2016.
- [35] A. Shabanpour-Haghighi, A. R. Seifi, T. Niknam, “A modified teaching - learning based optimization for multi-objective optimal power flow problem,” Energy Conversion and Management, Vol. 77, pp. 597-607, 2014.
- [36] S. Agrawal, B. Panigrahi, M. K. Tiwari, “Multiobjective particle swarm algorithm with fuzzy clustering for electrical power dispatch,” Evol Comput IEEE Trans, Vol. 12, pp. 529-541, 2008.
- [37] X. S. Yang, “Meta-heuristic optimization,” Scholarpedia, Vol. 6, 2011.
- [38] IEEE 39-Bus power system test cases, [Online], Available: http://electrica.uc3m.es/pablolle/varios_e.htm.
- [39] Wang, V. Vijay, K. Sun, “OBDD-based sectionalizing strategies for parallel power system restoration,” IEEE Trans Power Syst, Vol. 26, No. 3, pp. 1426-1433, 2011.

Appendix

The flowchart of whole mechanism of fuzzy based clustering is depicted in Fig. A, where N_{max} , S , $d_{c_{ij}}$, N_i and N_j show the maximum size of repository, current size of repository, the distance between two neighbor clusters (i, j), the number of solutions in clusters C_i and C_j , respectively [35].

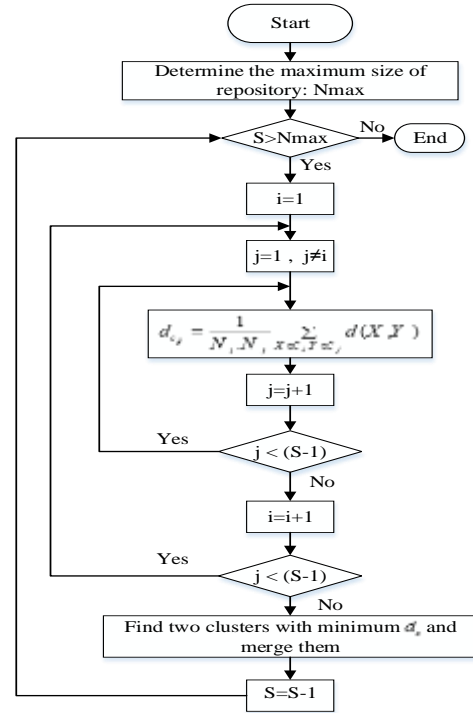


Fig (A): The flowchart of whole repository’s size controlling using fuzzy based clustering [35]

Nomenclature

P_{gi}	output active power of the i -th generator
P_{lj}	demand active power at d -th PQ bus
v_i	the actual value of the voltage for i -th PQ bus
v_j	the actual value of the voltage for j -th PQ bus
δ_{ij}	the difference value of phase angle between bus i and bus j
n	Number of generators
k	Number of PQ buses
Q_{gi}	output reactive power of the i -th generator
Q_{lj}	demand reactive power at d -th PQ bus
B_{ij}	the transfer susceptance between bus i and bus j
G_{ij}	the transfer conductance between bus i and bus j
V_{ref}	the value of the reference voltage
$V_{i_{min}}$	the lower voltage limit of i -th PQ bus
$V_{i_{max}}$	the upper voltage limit of i -th PQ bus
$P_{j_{max}}$	maximum output power for NBS unit j
$P_{j_{start}}$	required start-up power for NBS

	unit j
M	Total number of NBS units
$T_{j\min}$	certain time interval that NBS unit j need to be ready for receiving crank power
$T_{j\max}$	maximum time interval for starting the NBS unit j
$t_{j\text{path-opt}}$	time interval needed to energize the optimal path to NBS unit j
$P_{igen-opt}(t)$	generation capability of BS unit i for cranking the power through the optimal transmission path
t_{jstart}	Starting time of NBS unit j